Study of the crystal structure of todorokite by X-ray powder diffraction method

Hiroyuki Miura

Department of Geology and Mineralogy

Faculty of Science

Hokkaido University

Abstract

The x-ray powder diffraction data for todorokites was precisely studied and the crystal structure of todorokite is discussed. Three types of structure model are used to calculate the theoretical diffraction pattern. The layer structure model, the 3x3 tunnel model and the layer and bridge model were considered. It is obvious on comparing the experimental results of natural todorokite and the calculated results that the layer model agrees well with observed data. Weak diffraction peaks (d=6.9 Å and 4.4 Å) observed in todorokite are explained by the layer and bridge model which contains random H_2O between the [MnO_6] layers. These water molecules occupy the interlayer position. As the H_2O content in todorokite decreases on heating, the interlayer distance decrease. H_2O is a main constituent in the 'bridge' structure. Other elements such as Mn, Mg, Ca, O also form the bridge and stabilize the structure on heating. It is satisfactory to consider the structure of todorokite as a layer structure having a 'bridge' which connects each layer.

A Fourier map of acicular todorokite, which was calculated from rotation photographs, also shows the image of a layer structure. This structure is analogus to the layer structure of lithiophorite.

Content

Chapter 1. Introduction

Todorokite is a manganese oxide mineral having H_2O in its structure. It was reported at first from Todoroki gold mine, Hokkaido, Japan (Yoshimura,1934). This mineral is observed as aggregate of fine acicular crystals. MnO_2, H_2O, CaO, BaO and MgO are observed as main elements by chemical analysis. X-ray powder diffraction data of todorokite clearly show diffraction peaks of 9.6 Å, 4.8 Å, 3.2 Å, 2.45 Å and 1.42 Å.

Since 1934 there has been many reports of occurrence from all over the world (Frondel,1953; Frondel et al.,1960; Ljunggren,1960; Straczek et al.,1960; Faulring,1961; Lawrence,1962; Radtke et al.,1967; Lawrence et al.,1968; Harada,1982). There are many names for these type of minerals, such as "woodruffite" (Frondel,1953), "Delatorreite" (Straczek et al.,1960), "Buserite" (Giovanoli,1975). "10Å-manganite" (Buser,1959), which shows a similar x-ray diffraction profile to todorokite, and is the mineral observed in deep sea manganese nodules. There is confusion as to the definition of todorokite, with the main reason being that the crystal structure of todorokite has not been fully determined yet.

Buser and Grütter(1956) proposed that the crystal structure of todorokite in manganese nodule has a layer structure analogous to lithiophorite on the basis of x-ray diffraction profiles. However this idea has little support since lithiophorite can not contain Na^+ ions and the habit of cleavage is different from that of todorokite. Thus, instead of the layer model, the 3x3 tunnel structure model of todorokite was proposed on the basis

of crystal morphology (Burns and Burns,1977; Burns et al.,1983,1985). High resolution electron microscopic study of todorokite (Turner and Buseck,1981; Turner et al.1982; Siegel and Turner,1983) showed the tunnel imagery of crystal structure although there is still a problem with the tunnel structure model. The reasons for this are;

(1)the 3x3 tunnel model can not explain the x-ray powder diffraction data,

(2)the reduction of length of c-axis on heating can not be explained by a 3x3 tunnel model.

Structural correlation of lithiophorite with todorokite is unsatisfactory when crystal habits of todorokite and lithiophorite are compared (Burns and Burns,1977). However, this does not mean all layer structure models of todorokite are unsatisfactory. As the single crystal of todorokite is not available, we must study it by powder diffraction method. In this paper, the x-ray powder diffraction profiles based on three structure models were calculated and compared with the observed diffraction data from natural samples. X-ray diffraction photographs of acicular todorokite were obtained and the electron density distribution was calculated. Based on these data, the appropriate model for todorokite was discussed.

Chapter 2. Previous works

2-1. Classification of manganese dioxide minerals.

The fundamental crystal structure unit of manganese dioxide minerals is [MnO_6] octahedron. The [MnO_6] octahedron is linked by corner-sharing and edge-sharing to give variety of chain, tunnel and layer structures. All [MnO_6] octahedra are equivalent and share edges to form single, double and triple chains running parallel to the b-axis. The structure of some manganese dioxide minerals was proposed to have a tunnel structure based on chains of multiple edge-shared [MnO_6] octahedra. There are different ways of linkage of [MnO_6] octahedra in manganese dioxide minerals. Added complexities in the manganese dioxide arise from ordered and random vacancies in, and domain structures and non-periodic intergrowth of, the linked [MnO_6] octahedral units.

Possible crystal structure of manganese dioxides indicate that the classification of these minerals is derived from the basis of different linkages of [MnO_6] octahedra.

(a) Chain structure

The basis for describing the crystal structures of manganese dioxide minerals is the pyrolusite (β-MnO_2). It has a rutile (TiO_2) structure in which every Mn atom is surrounded by six oxygen atoms located at the vertices of a distorted octahedron with Mn at the center. The [MnO_6] octahedra share edges to form single chains extending along the c-axis (Fig.1-a). These chains influence the morphology of pyrolusite which frequently has an acicular habit. The single chains in pyrolusite are cross-linked with neighboring chains by corner-sharing of oxygen atoms of

adjacent octahedra. The hexagonally closed-packed oxygen layers along [100] are puckered to give tetragonal symmetry.

Ramsdellite has the same chemical formula to pyrolusite. This mineral contains double chains of linked [MnO_6] octahedra (Byström,1949). The octahedra are linked together by sharing opposite edges, thus producing continuous pyrolusite chains along the c-axis. Two such chains are cross-linked by edge sharing, one chain being displaced 1/2 c with respect to the other, so that an octahedron from one chain shares an edge with each of two octahedra from the other chain. The double chains of linked octahedra are further cross-linked to adjacent double chains through corner sharing of oxygen atoms, to give orthorhombic symmetry (Fig.1-b). The nsutite or γ-MnO_2 group consists of irregular structural intergrowth between pyrolusite and ramsdellite units. The alternating c-axis chain segments of the basic single- and double-chain units is random, so that no regular periodicity or superstructure is apparent.

(b) Tunnel structure

Minerals of hollandite-cryptomelane or α-MnO_2 group have structures based on that of ramsdellite (Byström and Byström, 1950;1951). This structure contains infinite double chains of edge-shared [MnO_6] octahedra. In hollandite minerals with tetragonal symmetry, these chains extend along the c-axis; whereas, in varieties with monoclinic symmetry the b-axis become the chain direction. The octahedron of the double chains share corners with adjacent double chains to give a three-dimensional framework containing large tunnels (Fig.1-c). This produces a

large cavity with accommodates large cations. General formula of α-MnO_2 group is described as $A_xMn_8O_{16}\cdot nH_2O$. They are named depending on the species of A-cation. Hollandite, cryptomelane, coronadite and manjiroite have the same structure and contain large cations such as Ba^{2+}, K^+, Pb^{2+}, Na^+ respectively. Generally Ba^{2+} ions and H_2O molecules occupy the tunnel site of the hollandite structure (Byström and Byström,1950,1951; Post et al. ,1982; Miura,1986). The non-stoichiometry and local charge balancing by large cations in the tunnel and voids of vacancies or Mn^{2+},Mn^{3+},etc.,in the [MnO_6] octahedra are significant factors which may contribute to exchange of the cations and fractionation of minor elements.

Psilomelane (Fig.1-d) has a tunnel structure analogous to hollandite (Wadsley,1953). It consists of triple chains of [MnO_6] octahedra linked by double (ramsdellite-like) chains to form a series of tunnels running along the b-axis. The b dimension of the psilomelane structure corresponds, therefore, to the c dimension of pyrolusite, ramsdellite and tetragonal hollandite-cryptomelane. The large tunnels are again occupied by Ba^{2+},K^+,H_2O,etc.,so that the psilomelane structure resembles the hollandite structure to which it breaks down at high temperature.

(c)Layer structure

Another important crystal structure of manganese dioxide minerals is layer type structure.

The crystal structure of chalcophanite ($ZnMn_3O_7\cdot 3H_2O$) consists of single sheets of water molecules between layers of edge-shared [MnO_6] octahedra, with Zn atoms located between the water layer and oxygens of the [MnO_6] layer (Wadsley,1955). The

stacking sequence along c-axis is thus -O-Mn-O-Zn-H_2O-Zn-O-Mn-O- and the perpendicular distance between two consecutive [MnO_6] layers is about 7.17 Å. The water molecules are grouped in open double hexagonal rings, while vacancies exist in the layer of linked [MnO_6] octahedra, so that six out of every seven octahedral sites are occupied by manganese. Each [MnO_6] octahedron shares edges with five neighboring octahedra and is adjacent to a vacancy. The Zn atoms are located above and below the vacancies in the manganese layer and are coordinated to three oxygens of the [MnO_6] layer. Each Zn atom completes its coordination with three water molecules so as to form an irregular coordination polyhedron.

Lithiophorite [$(Al,Li)MnO_2(OH)_2$] also has a layer structure (Wadsley,1952). The edge-shared [MnO_6] octahedra layers alternate with [$(Al,Li)OH_6$] octahedra layers. The stacking sequence along the c-axis is: -O-Mn-O-OH-(Al,Li)-OH-O-Mn-O-, and two consecutive [MnO_6] octahedra layers are about 9.5 Å apart. Vacancies occurring in the sheets of linked [MnO_6] octahedra in the chalcophanite structure are not characteristic of the linked [MnO_6] octahedral layers of lithiophorite, although vacancies may exist between the sheets.

Birnessite is also considered to have a layer structure. The crystal structure of a natural birnessite has not been determined, and information has been derived from electron diffraction measurements for synthetic compounds of the birnessite group (Giovanoli and Stahli,1970). Platelets of synthetic $Na_4Mn_{14}O_{27}\cdot 9H_2O$ and $Mn_7O_{13}\cdot 5H_2O$ were deduced to have a

structural model similar to chalcophanite. Thus sheets of water molecules and hydroxyl groups are located between layers of edge-shared [MnO_6] octahedron separated by about 7.2 Å along the c-axis. One out of every six octahedral sites in the layers of linked [MnO_6] octahedra is unoccupied, and Mn^{2+} or Mn^{3+} ions are considered to lie above and below these vacancies. These low-valence manganese ions are coordinated to oxygens in both the [MnO_6] layer and the (H_2O,OH) sheet. The position of sodium in the intermediate layer is uncertain. The electron micrographs of natural and synthetic birnessites show crystals with platey and lamellar habits which correlate with the proposed layer structure.

2-2. The X-ray powder diffraction data of todorokite

X-ray data of todorokites from several localities are compared in Table 1. It is apparent from the d-spacings in the table that considerable variation exists between relative intensities of comparable lines for different todorokite samples. In the data from Romaneche(France) and Huttenberg(Austria), the diffraction peak of 6.9-7.1 Å is observed, whereas in the data from other localities, this peak is not reported. As the d-spacing of (001) diffraction peak in birnessite is 7.2Å, it is not thought that the 6.9-7.1 Å peak observed in todorokite is caused by the presence of birnessite as an impurity. Todorokite from Farragudo(Portugal), (Frondel,1960) and from Vermlands Taberg(Ljunggren,1960) do not have this peak.

When the diffraction peak is weak and broad, it is very

difficult to distinguish the diffraction peak from the baseline and sometimes may be mistaken. Thus it is better to compare the data by diffraction profile than by d and I table.

In earlier studies, unit cell parameters were derived for todorokites from x-ray powder patterns. Straczek et al. (1960) found parameters of a=9.75 Å, b=2.84 Å, c=9.59 Å, and β =90° for a unit cell with either orthorhombic or monoclinic symmetry. Fauling (1961) found similar parameters of a=9.65 Å, b=10.29 Å, and c=2.84 Å with α, β and γ angles varying slightly from 90° for a sample from Charco Redondo,Cuba. The unit cell was considered to be pseudo-orthorhombic and triclinic. Many types of disorder are present in todorokites. The ubiquity of disorder explains the confusing x-ray diffraction patterns and hence the difficulty in determining structure types by x-ray diffraction measurements.

2-3. Early studies of todorokite structure.

The crystal structure of todorokite has not been determined mainly because single crystals suitable for a structural analysis have not been found. Buser and Grütter (1956) suggested that the structure of todorokite in manganese nodules has a layer structure analogous to lithiophorite, because prominent d-spacings around 9.6 Å and 4.8 Å for manganese nodules corresponded to similar basal spacings in the x-ray powder diffraction pattern of lithiophorite. However, synthetic experiments of lithiophorite by Giovanoli et al. (1973) showed that substantial amounts of Na^+ or other cations cannot be substituted in the lithiophorite structure. They concluded that lithiophorite differs fundamentally from todorokite. Crystals of

lithiophorite consist of laminae showing one perfect cleavage parallel to (001). This habit correlates with the layer structure determined for lithiophorite. Todorokite specimens, on the other hand, consist of fibrous aggregates of small needle-shaped crystals, resembling many specimens of cryptomelane, hollandite and psilomelane. Furthermore, electron micrographs of todorokite (Straczek et al.,1960;Hariya,1961) show that the crystals consist of narrow lathes or blades elongated along one axis (parallel to b) and showing two perfect cleavages parallel to the (001) and (100) planes. Minerals of the hollandite and psilomelane groups also show two perfect mutually perpendicular cleavages at right angles to the elongation of the acicular crystals. This resemblance suggests that todorokite has a crystal structure similar to that of hollandite and psilomelane and not that of lithiophorite (Burns and Burns,1977). The crystal structure model of todorokite was proposed by Burns and Burns(1977). They insist that todorokite resembles cryptomelane, hollandite and psilomelane in the following points. (1)It consists of an aggregate of fibrous crystal.(2)It has two perfect cleavages parallel to (001) and (100). On the basis of the above, they proposed the tunnel structure consisting of triple [MnO_6] chains (Fig.1-e), analogous to α-MnO_2. If todorokite does have a tunnel structure, then it is possible to have Mn^{2+} and Mn^{4+} ions in [MnO_6] chains and have large molecules in the tunnel site.

Recent work has been done on todorokites by a variety of techniques. Chukhrov et al.(1978;1979) observed the polymorphs of todorokite by selected area electron diffraction method. They

reported on todorokite with unit cell length of a=9.75, 14.6, and 24.38 Å, and classified the todorokite polymorph based on the length of a-axis. As the length of a-axis is a multiple of 4.88Å, they recommend the following nomenclature : todorokite I with a=4.88 Å, todorokite II with a=4.88 x 2 Å, todorokite III with a=4.88 x 3 Å, todorokite IV with a=4.88 x 4 Å and todorokite V with a=4.88 x 5 Å. Todorokite II,III, and V have already been found in nature.

Turner and Buseck(1981) reported that terrestrial todorokites consist of tunnel structures of previously unreported dimensions and that these tunnel structures are intergrown coherently on a unit cell scale. This todorokite family consists of related intergrowths of tunnel structures of size 3x3, 3x4, 3x5, and so forth, with the common triple chain. They pointed out that it has become apparent that a revised nomenclature is needed for the new structure of the todorokite family and, indeed, for the whole group of manganese oxide tunnel materials. Electron diffraction patterns with spacing of 9.75 Å, 14.6 Å and 24.4 Å in different samples of todorokite by Chukhrov et al.(1976) interpret these spacings to reflect predominant tunnel sizes 3x3, 3x5, and 3x9 respectively.

IR spectra of todorokite are consistent with either a layer structure of linked [MnO_6] octahedra containing vacancies, or a highly polymerized chain or tunnel structure with quadruple chains (Potter and Rossman, 1979). Modelling of the structure of todorokite is discussed by Burns and Stockman (1983). However, crystal structure of todorokite appear to contain variable linkages of edge-shared [MnO_6] octahedra and to be characterized

by numerous structural defects, essential cation vacancies in the chains or layers of linked octahedra, domain intergrowth of mixed periodicities, extensive atomic substitution (particularly divalent Ni, Cu, Zn, Mg, etc., for Mn^{2+}, and cation exchange properties. The problem is

(a) What is the main structure of todorokite ?

(b) Does 3x3 tunnel structure exist in todorokite ?

(c) Can the model structure explain the x-ray diffraction profile ?

(d) Does the structure change over the unit cell range ?

Chapter 3. Experimental method.

3-1. X-ray powder diffraction study.

An x-ray powder diffraction pattern of todorokite was studied in order to make a crystallographic characterization of this mineral. Samples were selected from 5 localities, Todoroki mine (Hokkaido), Ikeshiro mine (Shizuoka prefecture), Maruyama mine (Aomori prefecture), Urizukuri (Yamaguchi prefecture) and Akan-Yunotaki(Hokkaido). In the Todoroki mine, this mineral occurs as an aggregate of very fine flakes about 0.05 mm in length at the largest (Yoshimura,1934). It covers the wall of a druse in the oxidized zone of the gold deposit. The occurrence of the two samples from Maruyama mine and Ikeshiro mine are not known. Both of them are also aggregates of fine acicular crystals.

In Urizukuri, Yamaguchi prefecture, the todorokite occurs in the hydrothermal alteration zone. This sample does not show typical crystal habit. By electron micrograph, typical acicular form was observed (Harada,1982). Todorokite from Akan occurs in hot springs by recent volcanic activity. It looks like clay with black color. The x-ray powder diffraction data were collected using Cu-Kα radiation with a graphite monochromator from $2\theta=4^{\circ}$ to 70°. Step size was 0.05° and count time was 30 sec. Samples were fixed on the sample holder which was made of Si single crystal plate, to minimize the effect of background scattering of x-ray. The 19 Å peak ($2\theta=4.5^{\circ}$) was observed in the diffraction profiles of todorokite from Todoroki mine and Urizukuri. To closely examine the low angle diffraction peak,

samples which were fixed on the sample holder with preferred orientation were used. The sample with preferred orientation clearly shows the 19 Å peak.

3-2. Calculation of theoretical x-ray diffraction profile

To study what kind of crystal model can give the observed x-ray diffraction data, theoretical x-ray diffraction profiles based on some structure models were calculated. As mentioned above, Burns et al.(1977) proposed the 3x3 tunnel model consisting of [MnO_6] octahedron. On the other hand, Giovanoli(1985) argues against the tunnel model. In this paper, three models were selected for calculation of x-ray diffraction profile. They are "3x3 tunnel model", "layer model" and "layer and bridge model". It is assumed that the todorokite structure model consists of geometrically arranged [MnO_6] octahedron. The octahedron is a basic unit in many manganese oxide minerals and observed in the structure of pyrolusite, ramsdellite, hollandite and cryptomelane etc. The calculation program for "3x3 tunnel model" and "layer model" is written in BASIC on the basis of "PPDP" written by Ando and Kawahara(1982).

To explain the broad peaks, the layer and bridge model is considered. This model is a layer structure having H_2O molecule between the [MnO_6] layer at random.

The calculation program of diffraction profile for a random structure was written in FORTRAN. The subroutine CALC in UNICS program (Sakurai,1967) was modified and used for calculation of structure factors. Peak profile was drawn by Gaussian function.

3-3. Crystal structure analysis of acicular todorokite by x-ray diffraction method.

An x-ray diffraction photograph of acicular todorokite sample was taken. The acicular sample was set on the four circle x-ray goniometer as the long axis was kept in a vertical position (Fig.2). As the acicular todorokite is made of approximately parallel alignment, an x-ray diffraction photograph resembling rotation photograph is obtained. Graphite monochromated Mo-Kα radiation with 60 kv, 200 mA was used for the experiment. The distance between specimen and flat film was 30 mm (Fig.9-a) and 60 mm (Fig.9-b). The exposure time was 30 minutes. All axes of goniometer and film were fixed during exposure.

Chapter 4. Experimental results.

4-1. X-ray diffraction profiles of todorokite.

X-ray data for todorokites from Japan are compared in Table 2 and Fig.3. It is apparent that considerable variation exists between relative intensities of comparable lines for different todorokite samples. The maximum peak intensity varies with the crystallinity. Fig.4 also shows the x-ray diffraction profiles of the same samples using a step scanning method. The full scale of vertical axis is 100 cps. As the step size was 0.05 ^{o} and the count time per step was 30 sec, weak and broad peaks of todorokites were easily detected by this method. As shown in Fig.4, the 6.9Å and 4.4Å peaks are found in the diffraction data of todorokite from Todoroki, Ikeshiro, Maruyama and Urizukuri. Their peak intensity related to the maximum intensity peak are 1-2 %(6.9Å) and 2-8 %(4.4Å). The diffraction profiles of todorokite from Akan-Yunotaki do not show these diffraction peaks and this indicates that its structure is different from the todorokite from Todoroki mine, Ikeshiro mine, Maruyama mine and Urizukuri.

The unit cell data of each todorokite sample at room temperature are calculated using 5 diffraction peaks which are common in each sample (Table 3). The a and b parameters of each todorokite are almost constant whereas the c parameter varies widely. The length of c-axis changes on drying or heating (Harada,1982; Miura and Hariya,1984). The difference in c-parameters, observed in todorokite, is controlled by water content of the specimen.

4-2. Superstructure of todorokite.

Re-examination of x-ray powder diffraction data of todorokite from Todoroki mine and Urizukuri was carried out. Samples which have preferred orientation were used for the study. The diffraction peak of 19.3 Å (Table 4) was observed in the powder diffraction profiles of these two samples. No data have been reported on the d-spacing of larger than 9.6 Å. The d-spacing(19.3 Å) is twice that of 9.6 Å which is the strongest line in the diffraction data. When samples are fixed to the holder with preferred orientation, the peak of 19.3 Å becomes clear, as well as 9.6 Å and 4.8 Å. The 19.3 Å peak was assigned as todorokite basal plane (001). The unit cell parameters, refined by the least-squares method using 7 reflections of random orientation sample are;

$a=9.79 \pm 0.06$ Å, $b=2.86 \pm 0.01$ Å, $c=19.50 \pm 0.24$ Å.

Todorokite species may be characterized by unit cells having different parameters of c-axis. These todorokites are new species of superstructure. The relationship between the superstructure and polymorph of todorokite reported by Chukhrov et al.(1978,1979) will be discussed later.

4-3. Thermal study of todorokite.

The unit cell parameters of todorokite vary on heating. Fig.5 shows the unit cell dimensions of todorokite from Todoroki mine at each temperature. The c-axis diminishes in size considerably, whereas the a-axis and b-axis are constant. The

length of b-axis is 2.86Å, which resembles that of the unit cell length of other manganese oxide minerals. As this length corresponds to the ionic radii of oxygen, it is reasonable that the b-axis is constant on heating. The decrease in c-parameters starts with heating and ends at about 330 ^{o}C. The release of H_2O also ends at this temperature (Miura and Hariya,1984). a-parameter is almost constant and independent on heating. The difference of behavior on heating between a- and c-parameters show the difference of crystal structure along a- and c-axis of todorokite.

4-4. Calculated x-ray diffraction profile of the 3x3 tunnel model.

Most todorokites of hand specimen consist of fibrous aggregates of small acicular crystals. The crystal structure of todorokite has not been determined. Thus, any information has not been derived from experimental results. The method used in this investigation is based on comparing the calculated x-ray diffraction profile on the basis of model structure with that of natural samples. The crystal structure of manganese dioxide minerals consists of [MnO_6] octahedra, with the structure model for calculation also formed with these units. Suppose [MnO_6] octahedron which consists of 6 oxygen ions having 1.425 Å ionic radii are bonded to each other without distortion. Twice of the atomic radii of oxygen equals the length of the b-axis. The length of two edges of the tunnel is equal. The crystal system is

thus supposed to be tetragonal. The unit cell is shown in Fig.6-a. The setting of unit cell is analogous to α-MnO_2. The b-axis is located at the 4_2 axis following the tetragonal α-MnO_2. Consequently, the direction of crystal axis is identical to that of Straczek et al.(1960). There is a H_2O molecule or metallic ion in the tunnel of the structure model proposed by Burns et al.(1984). Crystal structure analysis data of α-MnO_2(Post et al.,1984,Miura,1986) showed that a metallic ion and H_2O occupy the tunnel site. In the calculation, tunnel ions are not considered for simplification. The crystallographic data used in the calculation is listed in Table 5. Table 6 and Fig.7 shows the calculated x-ray diffraction data of the todorokite model structure which has 3x3 tunnel, compared with natural todorokites from some localities. The calculated data is basically different from the observed data of natural todorokite in the following way; the diffraction peak of (00L) is observed in the calculated data, whereas the intensity of calculated diffraction peaks of 6.9Å and 4.4Å are not concordant with the observed data of natural todorokite.

4-5. Calculated x-ray diffraction profile of the layer model

One of the most important structural models of manganese dioxide minerals is the layer structure. This structure consists of layers of edge shared [MnO_6] octahedra. The layers of [MnO_6] octahedra separated by about 9.6 Å along the c-axis. The crystallographic data of the layer model used for calculation are listed in Table 7 and the structure model is shown in Fig.6-b.

Table 8 and Fig.7 shows the calculated data of the layer model. The calculated diffraction profile on the basis of the layer model is similar to the observed data from natural todorokites. It does not have a diffraction peak of 6.9Å nor 4.4Å which are observed in the diffraction data of 3x3 tunnel model. So it is reasonable to recognize that the todorokite from Todoroki mine, Ikeshiro mine, and from other localities in Japan may have a layer structure generally.

4-6. Calculated x-ray diffraction profile of the layer and bridge model.

The layer and bridge model is supposed to explain the broad peaks observed in natural todorokite. This model is a layer structure with enclosed sheets of H_2O molecule between the [MnO_6] layer. Todorokite contains a significant amount of H_2O in its structure, and it is considered that H_2O is essential to todorokite structure. H_2O molecule is arranged at position A(0,0,0.5) or position B(0.5,0.5,0.5) at random (Fig.6-c). The positions of H_2O in 200 unit cells which lined up to a-axis were determined using random numbers (Table 9). In the calculation, the atomic scattering factor of oxygen is used for H_2O. The calculated diffraction profile is shown in Fig.8. To compare the weak and broad peaks, vertical scale is magnified. The layer and bridge structure which contains bridge at random can explain the broad and weak diffraction peaks observed in natural todorokite.

4-7 X-ray diffraction photograph of acicular todorokite.

The x-ray diffraction photographs of acicular todorokite from Todoroki mine are shown in Fig.9. If the specimen is a single crystal, the diffraction spot would not be observed on the film. The rotation of specimen is necessary to set the appropriate position for diffraction. If the specimen is aggregate of fine powder crystals with random orientations, the photograph will show concentric Debye-Scherrer rings. The x-ray diffraction photograph shows weak Debye-Scherrer rings and diffraction spots. The debye-rings were derived from fine powder crystals of random orientations and the spots were derived from fibrous todorokite crystals. To obtain this type of diffraction photograph, rotation of the specimen is necessary. If the specimen consists of many fibrous crystals parallel to a certain axis and another two axes of fibrous crystals are set in random directions, the same rotational effects will occur. So, it is natural to consider that the specimen is aggregate of fibrous crystals parallel to a certain axis. Thus it is possible to treat the photograph as a rotation photograph. The distance between the zero layer and 1st layer reveals that the unit cell, which is constant along the extended axis of acicular todorokite, is 2.8 Å. The specimen elongates along the b-axis.

Each spot was indexed by the following manner. Assuming the cell constants as a=9.76 Å, b=2.87 Å, c=9.68 Å, $\alpha=90^{o}$, $\beta=90^{o}$, $\gamma=90^{o}$,then the d-value of each indexes may be calculated. The distribution of diffraction spots on film had a center of symmetry, and the value of tan(2θ) is available by dividing

half of the distance between the corresponding diffraction spots by the distance between the specimen and film. From these data, observed d-values were obtained. Assuming the spots on the zero layer have a index of (h0l) and the spots on the 1st layer have a index of (h1l), then indexes can be determined comparing the calculated d-spacing and the observed d-spacing.

The intensity of the spots were calculated on the basis of the peak area which was measured by photometer. Multiplicity of diffraction were considered in calculating the intensity of the diffraction peak. For example, the intensity of diffraction spot (001) in Fig.9 is affected by (001) and $(00\bar{1})$. The multiplicity is 2. As the spot (101) is a superpositional spot for (101),$(10\bar{1})$,$(\bar{1}01)$,$(\bar{1}0\bar{1})$, the multiplicity is 4. The diffraction intensity of each peak was obtained by dividing observed intensity by multiplicity. As an orthorhombic system was assumed, structure factors of hkl,hk$\bar{l}$,$\bar{h}$kl,$\bar{h}$k$\bar{l}$ are equivalent. Table 5 shows the index, calculated d-spacings, observed d-spacings and intensity. Unfortunately, a few spots could not be indexed by this method. This may be because of disorder in the specimens of todorokite. In this study, these spots are ignored.

Based on the above intensity and the phase derived from 3x3 tunnel model, Fourier synthesis was performed. RSSFR-5 in UNICS system (Sakurai,1967) was used for calculation. Four peaks of high density and 10 peaks of low density were observed in the Fourier map. It was assumed that high density peaks were manganese and others were oxygen atoms. The final result is shown in Fig.10 as a projection on (010). No large residual peak were observed in the differential Fourier map. Four high electron

density peaks are observed at c=0 and c=0.5. They elongate in the a-axis direction and indicate the position of the sheets of Mn. The presence of oxygen atoms surrounding the Mn atom are not clear from this figure. Between the Mn layers which exist at 9.6 Å spacings, an additional layer exists. The electron density of this layer is lower than the Mn layer.

5. Discussion

5-1. The structure model of todorokite.

The intensity of x-ray diffraction peaks of high order are affected significantly by atomic coordinates or temperature factors. However the intensity of low order peaks are not affected by these factors and they show the features of the fundamental structure. In this study, the data of low angle peaks ($2\theta < 30^{o}$) were used for discussion. The comparison of the theoretical x-ray diffraction profiles of todorokite and the observed profile shows that todorokite has a layer structure. The 3x3 structure model can not explain the observed profile. For the weak peaks in the observed data, it is possible to explain by the layer and bridge model which contains H_2O between [MnO_6] layers at random. The weak and broad diffraction peak of 6.9 Å and 4.4 Å shows the existence of bridge which connect each [MnO_6] layer. The elements which form the bridge are different from the [MnO_6] layer which contains H_2O.

Heat treatment of todorokite also shows that the todorokite has a layer feature. The d-spacing of the (00L) diffraction peaks of todorokite from Urizukuri decreases when dried (Harada,1982). Todorokite from Todoroki mine also has decreased d-spacing of (00L) diffraction peaks on heating. If todorokite has a 3x3 tunnel structure and the arrangement of [MnO_6] octahedron is the same for both a-axis and c-axis, a-axis should contract simultaneously. However the observation results show only c-axis contracts on heating. The structure of todorokite is different in a- and c-axis directions. The

difference between the tunnel structure and the layer structure is a result of whether the nature of layer and bridge is different or not. As H_2O exists in the bridge, the layer and bridge are different in todorokite. From this point of view, todorokite has a layer structure. The bridge can not be formed by H_2O molecules alone. It consists of various kinds of elements and has definite structure but the detail of the bridge is not clear yet. Todorokite has irregularity in its structure and it must be recognized that these irregularities are the nature of todorokite.

A Fourier map of acicular todorokite also shows the layer image. It is not possible to solve the structure with high accuracy because the observed data contains some errors. For example, (a)the number of observed diffraction peaks were insufficient, (b)film factors were not corrected, (c)the sample contains superstructure, (d)the c-axis of each crystal was not completely parallel. However it will show the image of todorokite structure. The Fourier map, projected on (010), shows the high electron density layer existing in todorokite. The layer exists at 9.6 Å intervals and between these layers, other layers exist. The Fourier synthesis map of todorokite is quite similar to the crystal structure of lithiophorite (Wadsley,1952).

5-2. Superstructure of todorokite.

The broadness of the x-ray diffraction peaks of 6.9 Å and 4.4 Å are explained by disorder in the position of the bridge. The arrangement of the bridge will orientate the superstructure towards the a-axis. In a structure of well crystallized todorokite, bridges will exist at regular intervals. Fig.11 shows the schematic diagram of the layer and bridge structure model having different intervals of bridge. A small square represents [MnO_6] octahedron. Each octahedron shifts 1/2 b alternately as figured by white and black square. The length of one [MnO_6] in the direction of a-axis is 2.47 Å. If bridges exist at every 5 [MnO_6], bridges shift 1/2 b alternately depending on the position of [MnO_6] in layer (Fig.11-b). So 12.3(=2.47x5) Å should not be the length of a-axis. If bridge exist at every 7 or 9 [MnO_6], 17.3(=2.47x7) Å or 22.2(=2.47x9) Å will not be an a-axis in a similar manner. In this model, the length of a-axis is multiples of 4.94(2.47x2) Å. The polymorph of todorokite reported by Chukhrov et al.(1978) is possible to explain by this model.

The superstructure observed in todorokite from Todoroki mine is different from the superstructure reported by Chukhrov et al.(1978). A small fragment of todorokite crystal has a plate shape flattened on (001). The relationships between the crystal morphology and crystal axis is shown in Fig.12 after Straczek et al.(1960). The direction of superstructure reported by Chukhrov et al.(1977,1978) is vertical to c-axis. In an electron diffraction study, an electron beam hits flat specimens vertically and the diffraction pattern shows symmetry which

obeys the arrangement of atoms in a plane vertical to the c-axis. Whereas the direction of superstructure observed by x-ray powder diffraction study of todorokite from Todoroki mine and Urizukuri using preferred orientation specimen, is parallel to c-axis as mentioned above. Todorokites have two types of superstructure in different directions. The superstructure toward a-axis is derived from the disordered arrangement of bridge. And the superstructure toward c-axis is derived from the stacking of [MnO_6] layer.

Crystal habit of todorokite can possibly be explained through this model. As todorokite has a layer structure parallel to (001), flake of todorokite exhibit a flat shape. There is a disorder towards a-axis and cleavage exists parallel to the (100) plane. The nature of these two cleavages are different. So the shape of a todorokite crystal is narrow lath or blade elongated along b-axis.

5-3. Crystallization process of natural todorokite

Todorokite from Akan contains a significant amount of water. It releases water and deforms at very low temperatures (Miura and Hariya,in print). The x-ray diffraction data does not show the existence of bridge. This means H_2O exists between the layers completely at random.

From the above data, the following process can explain the formation of todorokite. At first a layer of [MnO_6] is formed. Many kinds of ions such as Ca, Mg, Na etc and H_2O exist between layers and make 9.6-10 Å separation. These ions and H_2O

exist completely at random and are fixed to the layer loosely. So, H_2O is released at very low temperature and the distance between each layer decreases. Finally, the structure deforms. As interlayer ions and H_2O exist at random, the diffraction peak of 6.9 Å and 4.4 Å are not observed by x-ray powder diffraction. Todorokite from Akan is at this stage. These ions and H_2O are fixed in the stable position and unstable H_2O will be released gradually. At this stage x-ray diffraction peaks of 6.9 Å and 4.4 Å are observed as the interlayer ions and H_2O molecules occupy the special position.

Chapter 6. Conclusions

From the present experimental study, the following conclusions are obtained.

(a)Theoretical x-ray diffraction profile calculation based on the layer and tunnel model reveals that the basic structure of todorokite is layer structure.

(b)Fourier synthesis map of acicular todorokite from Todoroki mine shows layer structure.

(c)The precise study of x-ray diffraction profiles of todorokite from Japan,including Todoroki mine, shows 6.9Å and 4.4 Å diffraction peaks.

(d)These diffraction peaks are explained by the presence of a bridge which connect each [MnO_6] layer at random.

(e)The superstructure of todorokite was observed along (001).

(f)The layer structure model is suitable for heat treatment of todorokite.

(g)The irregularity in structure is a main characteristic of todorokite.

Acknowledgments

The author wishes to express his sincere gratitude to Professor Yu Hariya of Hokkaido University for discussion on the subject and for his critical reading of the manuscript. He is also indebted to Drs. S. Yui, K. Togari and K. Kodaira for their helpful discussions.The author also thanks Dr. K. Sakurai for the samples from Ikeshiro and Maruyama which were sent to Professor Hariya. Thanks are also due to Professor G. Shibuya of Yamaguchi University for his help on the study of todorokite from Urizukuri.

References

Ando,Y. and Kawahara,A.(1982).A simplified X-ray diffraction profile drowing program,Ann.Meet.Miner.Soc.Japan.1982,Abstr., P-10.

Burns,R.G. and Burns,V.M.(1977).Mineralogy of manganese nodules. In G.P.Glasby,Ed.,Marine Manganese Deposits,p.185-248.Elsevier Publising Company,New York.

Burns,R.G.,Burns,V.M. and Stockman,H.W.(1983).A review of the todorokite-buserite problem:implications to the mineralogy of marine manganese nodules,Am.Mineral.,68,972-980.

Burns,R.G.,Burns,V.M. and Stockman,H.W.(1985).The todorokite-buserite problem:further considerations,Am.Mineral.,70,205-208.

Buser,W.(1959).The nature of the iron and manganese compounds in manganese nodules. In,M.Sears (ed.),Internat.Oceanogr. Congr.,AAAS,p.962-963.

Buser,W. and Grütter,A.(1956).Uber die natur der manganknollen. Schweiz.Min.Petr.Mitt.,36,49-62.

Byström,A.M.(1949).The crystal structure of Ramsdellite, an orthorhombic modification of MnO_2,Acta Chemica Scandinavica,3,163-173.

Byström,A. and Byström,A.M.(1950).The crystal structure of hollandite,the related manganese oxide minerals,and α-MnO_2,Acta cryst.,3,146-154.

Byström,A. and Byström,A.M.(1951).The positions of the barium atoms in hollandite,Acta Cryst.,4,469.

Chukhrov,F.V.,Gorshkov,A.I.,Sivtsov,A.V. and Beresovskaya,V.V. (1978).Structural varieties of todorokite.Izvestia Akademia Nauk,S.S.S.R.,Series Geology,12,86-95.

Chukhrov,F.V.,Gorshkov,A.I.,Sivtsov,A.V. and Beresovskaya,V.V. (1979).New data on natural todorokites,Nature,278,631-632.

Fauling,G.M.(1961).A study of cuban todorokite,Advance in X-ray Analysis,5,117-126.

Frondel,C.(1953).New manganese oxides:hydrohausmannite and woodruffite,Am.Miner.,38,761-769.

Frondel,C.,Marvin,V.B. and Ito,J.(1960).New occurrence of todorokite,Am.Miner.,45,1167-1173.

Giovanoli,R. and Stahli,E.(1970).Oxide und Oxihydroxide desdrei- und vier- wertigen mangans.Chimia,24;49-88.

Giovanoli,R.,Buhler,H. and Sokolowska,K.(1973).Synthetic lithiophorite:electron microscopy and x-ray diffraction, J.Microscopie,18,271-284.

Giovanoli,R.,Bruki,P.,Giuffredi.M. and Stumm,W.(1975). Layer structured manganese oxide hydroxides.IV.The buserite Group;structure stabilization by transition elements. Chimia,29,517-520.

Giovanoli,R.(1985).A review of the todorokite-buserite problem: implications to the mineralogy of marine manganese nodules: discussion,Am.Miner.,70,202-204.

Harada,S.(1982).Todorokite from Urizukuri,Kamikawa-mura,Abu-gunn,Journ.of Geol.Soc.of Yamaguchi Pref.10,1-6.(in Japanese)

Hariya,Y.(1961).Mineralogical studies on manganese dioxide and hydroxide minerals in Hokkaido,Japan,Journ.Fac.Sci. Hokkaido Univ.Ser.IV,10(4),641-702.

Larson,L.T.(1962).Zinc-bearing todorokite from Philipsburg, Montana,Am.Miner.,47,59-66.

Lawrence,L.J.,Bayliss,P. and Tonkin,P.(1968).An occurrence of todorokite in the deuteric stage of a basalt,Miner.Mag.,36, 757-760.

Ljunggren,P.(1960).Todorokite and pyrolusite from Vermlands, Sweden,Am.Miner.,45,235-238.

Miura,H. and Hariya Y.(1984).Todorokite with long spacing and structure of manganese dioxide minerals,Journ.Miner.Soc.Japan, 16,301-308.(in japanese with english abstract)

Miura,H.(1986).The crystal structure of hollandite,Miner.Jour., 13,119-129.

Post,J.E.,Dreele,V.D. and Buseck,P.R.(1982).Symmetry and cation displacements in hollandites:Structure refinements of hollandite, cryptomelane and Priderite,Acta Cryst.,B38,1056-1065.

Potter,R.M. and Rossman,G.R.(1979).The tetravalent manganese oxides:identification,hydration and structural relationships by infrared spectroscopy,Am.Miner.,64,1199-1218.

Radtke,A.S.,Taylor,C.M. and Hewett,D,F.(1967).Aurorite,Argentian todorokite and hydrous silver-bearing lead manganese oxide, Econ.Geol.,62,186-206.

Sakurai,T.(1967).Universal Program System for Crystallographic Computation,Cryst.Soc.Japan.

Siegel,M.D. and Turner,S.(1983).Crystalline todorokite associated with biogenic debris in manganese nodules,Science,219, 172-174.

Straczek,J.A.,Horen,A.,Ross,M. and Warshaw,C.M.(1960).Studies of the manganese oxides.IV.todorokite,Am.Miner.,45,1174-1184.

Turner,S. and Buseck,P.R.(1981).Todorokite:A new family of naturally occurring manganese oxides,Science,212,1024-1027.

Turner,S.,Siegel,M.D. and Buseck,P.R.(1982).Structural feature of todorokite intergrowth in manganese nodules,Nature,296, 841-842.

Wadsley,A.D.(1952).The structure of Lithiophorite $(Al,Li)MnO_2(OH)_2$, Acta Cryst.,5,676-681.

Wadsley,A.D.(1953).The crystal structure of psilomelane, $(Ba,H_2O)_2Mn_5O_{10}$,Acta Cryst.,6,433-438.

Wadsley,A.D.(1955).The crystal structure of chalcophanite, $ZnMn_3O_7 \cdot 3H_2O$,Acta Cryst.,8,165-172.

Yoshimura,T.(1934)."Todorokite",a new manganese mineral from the Todoroki mine,Hokkaido,Japan, Journ. Faculty Sci. Hokkaido Imp.Univ.,Ser IV,2,289-297.

Table 1. Selected x-ray powder diffraction data of todorokite.

Farragudo[1] Portugal		Charco Redondo[1] Cuba		Todoroki[1] Japan		Huttenberg[1] Austria		Romaneche[1] France		Philipsburg[2] USA		Ardglen[3] Australia		Aurora mine[4] USA	
I	d	I	d	I	d	I	d	I	d	I	d	I	d	I	d
10	9.56	10	9.60	10	9.68	10	9.60	10	9.58	10	9.6	8	9.4	10	9.43
------		1/4d	7.13	1/4d	7.15	3	7.02	2	6.98	1d	7.0	4	7.17	1	6.75
8	4.80	8	4.80	8	4.80	8	4.79	8	4.79	6	4.8	10	4.74	4	4.76
------		1d	4.45	1/2d	4.45	------		------		1d	4.45	1d	4.30	<1	4.48
------		------		------		1	3.48	3	3.48	------		------		------	
------		1/2d	3.40	------		------		------		------		------		------	
4	3.19	1	3.20	3/2	3.22	1/2	3.21	1	3.22	1	3.20	1	3.19	1	3.20
1/2	3.11	1	3.10	------		3	3.10	------		------		------		5	3.11
------		------		------		------		1/2d	2.98	------		------		------	
------		------		------		------		1/2d	2.88	------		1	2.79	d	2.66
------		------		------		------		------		------		3	2.49	1	2.49
2	2.46	3	2.46	2	2.46	2	2.46	------		2	2.46	------		2	2.45
4	2.40	5	2.40	4	2.39	5	2.40	4	2.41	4	2.405	3d	2.40	3	2.40
3	2.34	4	2.34	3/2	2.34	2	2.33	2	2.36	1	2.34	3	2.28	<1	2.35
3	2.23	2	2.23	2	2.22	2	2.23	3	2.19	2	2.22	------		------	
------		1/2d	2.13	1/2d	2.15	2	2.15	1/4	2.15	------		------		1	2.16
3	1.98	2	1.98	2	1.98	1	2.00	------		2	1.99	2	1.97	<1	1.995
2	1.93	1/2	1.92	1/2	1.92	------		------		------		------		<1	1.914
------		-------		------		------		1/2	1.83	------		2	1.89	------	
1	1.78	1	1.78	------		------		------		------		------		------	
1	1.74	1	1.74	1	1.75	1/4d	1.73	------		1/2	1.75	------		<1	1.756
------		1/2	1.68	------		------		------		------		4	1.69	<1	1.691
------		------		------		------		------		------				1	1.630
	1.54	1	1.53	1/2	1.54	1	1.55	1/2	1.56	1	1.54			<1	1.593
------		3	1.49	------		------		------		------				1	1.471
------		------		------		------		------		------				1	1.456
3	1.42	2	1.42	3	1.42	4	1.43	1	1.43	3	1.42			2	1.428
2	1.39	1	1.39	1	1.39	1/2	1.40	1/4	1.40					------	
														1	1.362
														<1	1.348

d=diffuse line

1 Frondel et al. (1960)

2 Larson (1962).

3 Lawrence (1960).

3 Radtke et al.(1967).

Table 2. X-ray powder diffraction data of todorokite from Japan.

Ikeshiro		Todoroki		Maruyama		Urizukuri		Akan	
I	d	I	d	I	d	I	d	I	d
100	9.57	100	9.67	100	9.60	100	9.56	100	9.74
1d	7.17	1d	7.20	<1d	7.20	2d	7.22	------	
20	4.78	15	4.82	20	4.78	23	4.78	25	4.89
2d	4.42	2d	4.45	3d	4.37	8d	4.43	------	
2	3.39	------		------		------		------	
6	3.17	3	3.21	5	3.17	5	3.23	2	3.25
11	3.11	2	3.10	5	3.08	5	3.12	------	
2	3.00	------		3	2.98	------		------	
------		------		<1	2.81	------		------	
<1	2.76	------		<1	2.77	------		------	
<1	2.62	------		<1	2.59	------		<1	2.55
2	2.45	2	2.44	3	2.44	11	2.45	12	2.44
5	2.40	5	2.40	8	2.39	16	2.39	------	
5	2.35	------		6	2.35	------		------	
1	2.21	<1	2.21	1	2.21	3	2.20	<1	2.22
<1	2.11	<1	2.16	<1	2.15	1	2.13	------	
------		------		<1	2.10	------		------	
2	1.97	<1	1.98	2	1.98	1	1.98	------	
<1	1.90	<1	1.91	1	1.91	<1	1.90	------	
1	1.78	------		2	1.77	------		------	
1	1.74	<1	1.75	2	1.74	<1	1.74	------	
<1	1.67	<1	1.67	<1	1.68	------		------	
<1	1.62	------		<1	1.65	------		------	
2	1.56	------		------		------		------	
<1	1.53	<1	1.54	1	1.53	<1	1.53	------	
<1	1.48	------		<1	1.48	------		1	1.46
1	1.42	1	1.42	1	1.42	1	1.42	4	1.42
1	1.39	<1	1.39	1	1.41	------		------	
<1	1.37	------		2	1.38	1	1.37	------	

d:diffuse line

Table 3. Unit cell constants of todorokite from Japan.

	Ikeshiro	Todoroki	Maruyama	Urizukuri	Akan
a(Å)	9.86(2)	9.877(6)	9.88(2)	9.86(4)	9.878(9)
b(Å)	2.824(7)	2.806(3)	2.806(9)	2.82(2)	2.806(4)
c(Å)	9.53(2)	9.635(7)	9.53(2)	9.64(4)	9.76(1)
V(Å^3)	265.2(9)	267.1(4)	264.2(11)	268.4(23)	270.5(5)

Table 4. X-ray powder diffraction data of todorokite having superstructure from Todoroki mine.

d	I	h k l
19.3	1	0 0 1
9.69	10	0 0 2
4.83	5	0 0 4
4.48	2	
3.22	2	0 0 6
2.46	5	0 1 4
2.40	6	0 0 8
2.35	3	
2.23	1	2 1 4
1.99	2	3 1 4
1.76	1	
1.54	1	
1.42	2	0 2 0

Radiation:Cu-Kα ,35Kv,20mA.
Monochromater:graphite.
Samples are fixed to the holder with preferred orientation.

Table 5. Crystallographic data of 3X3 model used for theoretical calculation.

Crystal system : Tetragonal
Space group : $P4_2/m$

Atomic coordinate

	x	y	z
Mn 1	0.113	0.500	0.365
Mn 2	0.250	0.000	0.250
Mn 3	0.387	0.500	0.135
O 1	0.122	0.000	0.468
O 2	0.105	0.000	0.263
O 3	0.259	0.500	0.353
O 4	0.241	0.500	0.147
O 5	0.395	0.000	0.238
O 6	0.378	0.000	0.032

Cell Constant

a = 13.81 Å
b = 2.85 Å
c = 13.81 Å
V = 543.7 $Å^3$

Formula MnO_2
Z = 12
D_{calc} = 3.19 g/cm^3

Table 6. Calculated results of x-ray powder diffraction data based on the 3x3 tunnel model.

2 Θ(Cu-Ka)	I	d	h	k	l
9.05	100	9.767	1	0	1
12.82	39	6.906	2	0	0
18.17	10	4.883	2	0	2
20.33	17	4.368	3	0	1
25.80	4	3.453	4	0	0
27.39	1	3.256	3	0	3
28.91	5	3.088	4	0	2
33.07	5	2.709	5	0	1
36.50	7	2.461	2	1	2
36.81	3	2.442	4	0	4
37.69	16	2.387	3	1	1
37.98	2	2.369	5	0	3
39.13	3	2.302	6	0	0
41.06	4	2.198	4	1	0
41.34	3	2.184	6	0	2
46.24	13	1.963	5	1	1
46.49	3	1.953	7	0	1
51.00	1	1.791	6	1	0
52.81	7	1.733	6	1	2
53.04	5	1.727	8	0	0
54.81	2	1.675	8	0	2
58.01	2	1.590	6	1	4
60.51	4	1.530	7	1	3
65.50	2	1.425	0	2	0
66.10	2	1.413	6	1	6
66.88	6	1.399	7	1	5
67.85	1	1.381	10	0	0 : 8 0 6
69.37	1	1.355	3	2	1

Table 7. Crystallographic data of layer model used for theoretical calculation.

Crystal system : Orthrhombic

Atomic coordinate

	x	y	z
Mn 1	0.000	0.000	0.000
Mn 2	0.250	0.500	0.000
Mn 3	0.500	0.000	0.000
Mn 4	0.750	0.500	0.000
O 1	0.083	0.500	0.879
O 2	0.167	0.000	0.121
O 3	0.333	0.000	0.879
O 4	0.417	0.500	0.121
O 5	0.583	0.500	0.879
O 6	0.667	0.000	0.121
O 7	0.833	0.000	0.879
O 8	0.917	0.500	0.121

Cell Constant

a = 9.87 Å
b = 2.85 Å
c = 9.60 Å
V = 270.1 $Å^3$

Formula MnO_2

Z = 4

D_{calc} = 2.14 g/cm^3

Table 8. Calculated results of x-ray powder diffraction data based on the layer model.

2 Θ(Cu-Ka)	I	d	h	k	l	
9.12	100	9.700	0	0	1	
18.29	10	4.857	0	0	2	
27.59	1	3.233	0	0	3	
36.40	2	2.468	4	0	0	: 2 1 0
37.61	6	2.392	4	0	1	
41.03	7	2.200	4	0	2	
46.28	6	1.962	4	0	3	
52.94	4	1.730	4	0	4	
60.72	2	1.525	4	0	5	
65.51	1	1.425	6	1	0	
66.30	1	1.410	6	1	1	
68.65	1	1.367	6	1	2	
69.51	1	1.352	4	0	6	

Table 9. Starting data for calculation of layer and bridge model

probability of A after A : 0.7
probability of B after B : 0.7
number of A : 95
number of B : 105
number of atoms : 2600
unit cell a : 1974.0 Å
b : 2.85 Å
c : 9.60 Å

Sequence of atomic position

A A A A A A A A A A B B B B B B B B A A
A A A B B A B A B B A A A B B B B A A A
A B B B A A A A A A A A A A A B B B B B
A A A A A A B A A B B B B B B A A A B B
B A A B A A B A A A A B B A B B B B B B
B A B A A A A A A A B B B B A B B B B B
B B A B B A B B B B B B B A A B B A A B
B A A B B B B B B B A A A A B B A B B B
B B A A A A A A A B A A A A B B B B B B
B A B A A A A B B B B B B B B B B A A

Table 10. X-ray diffraction data of acicular todorokite.

h	k	l	$2\theta_{obs.}$	$d_{obs.}$	$d_{calc.}$	I
0	0	1	4.2	9.72	9.69	14
1	0	1	5.6	7.23	6.89	3
0	0	2	8.4	4.84	4.85	28
1	0	2	9.4	4.34	4.34	12
0	0	3	12.9	3.16	3.23	46
0	0	4	16.8	2.43	2.42	29
1	0	4	17.3	2.36	2.35	14
2	0	4	19.4	2.11	2.17	11
1	0	5	21.6	1.89	1.90	6
4	0	4	23.3	1.76	1.72	16
0	0	6	25.0	1.64	1.65	64
6	0	5	32.5	1.27	1.25	11
0	0	8	34.4	1.20	1.21	22
1	1	2	16.9	2.40	2.39	100
2	1	2	18.6	2.19	2.20	14
3	1	2	20.7	1.97	1.97	42
4	1	2	23.7	1.73	1.74	50
2	1	5	27.2	1.51	1.52	32
1	1	6	29.5	1.39	1.39	77
0	2	2	30.7	1.34	1.37	72
3	2	2	32.3	1.27	1.26	28
2	2	4	34.4	1.20	1.19	68

Radiation:graphite monochromated Mo-$K\alpha$.

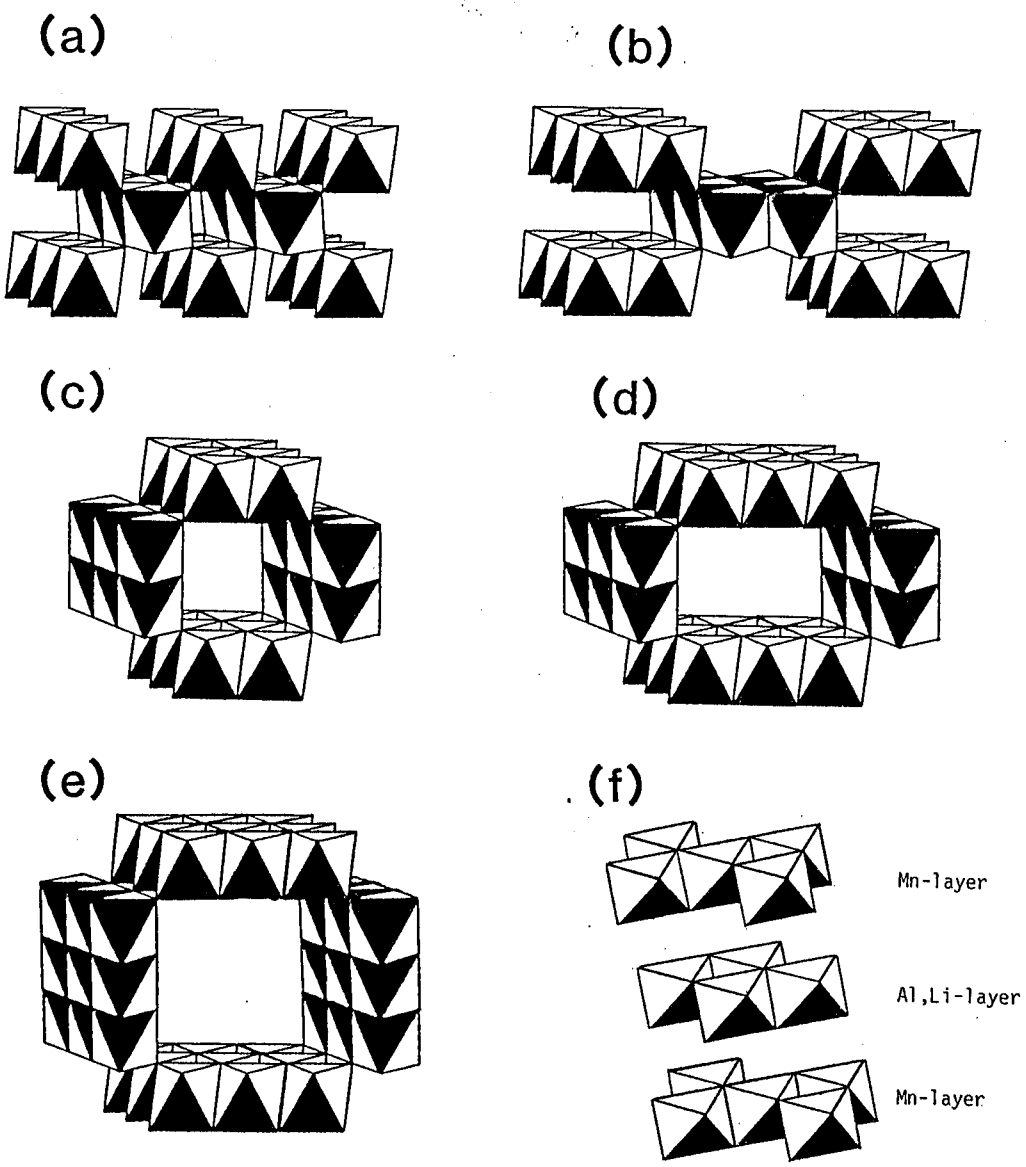

Fig.1 Diagram of various manganese oxide structures.

(a) pyrolusite
(b) ramsdellite
(c) hollandite
(d) psilomelane
(e) 3x3 tunnel structure
(f) lithiophorite

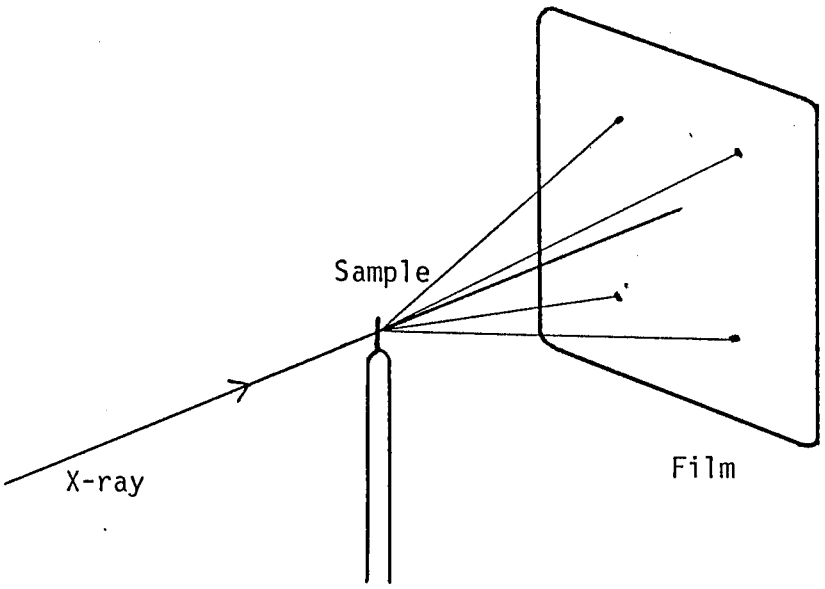

Fig.2 Experimental arrangement for taking photograph on a flat-plate film.

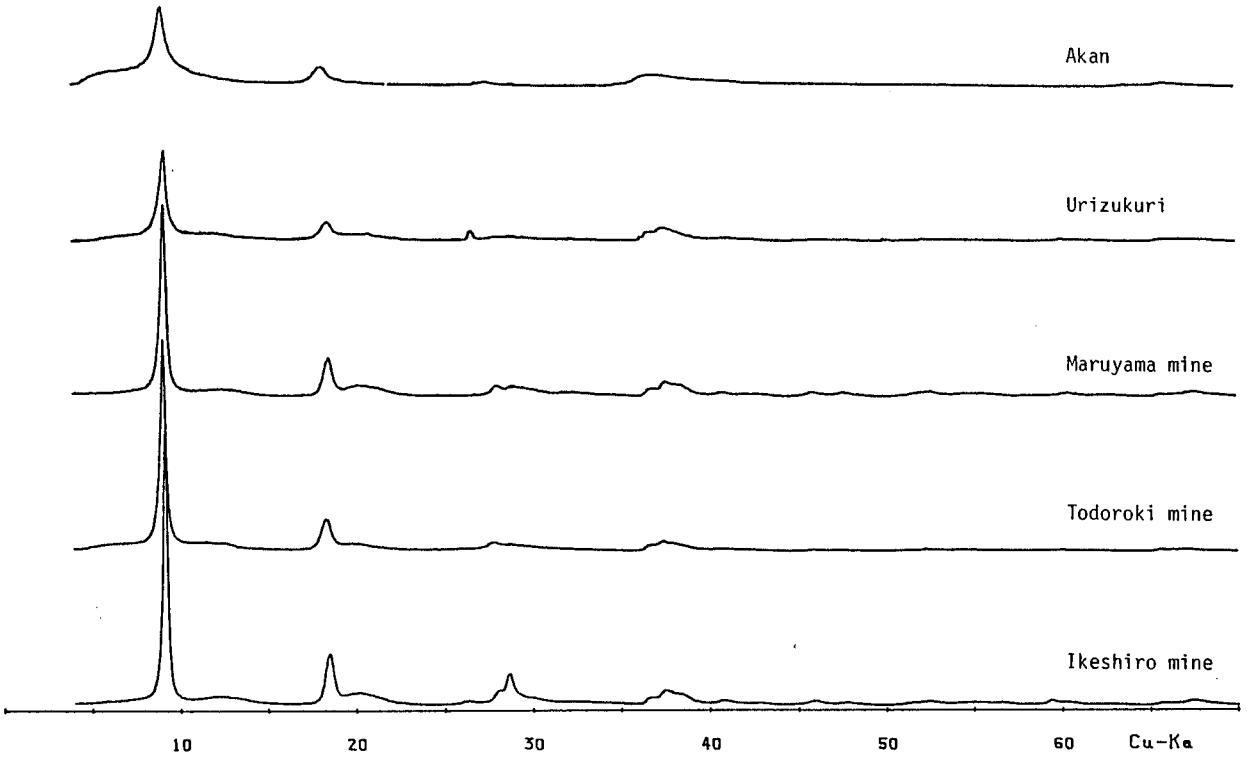

Fig.3 X-ray powder diffraction profiles of todorokite from Japan.
Experimental conditions.
Radiation: Cu-Kα , 35 Kv,20 mA,
Monochromater: graphite.
Scanning method: step scan, step size: 0.05°
Count time: 30 sec.

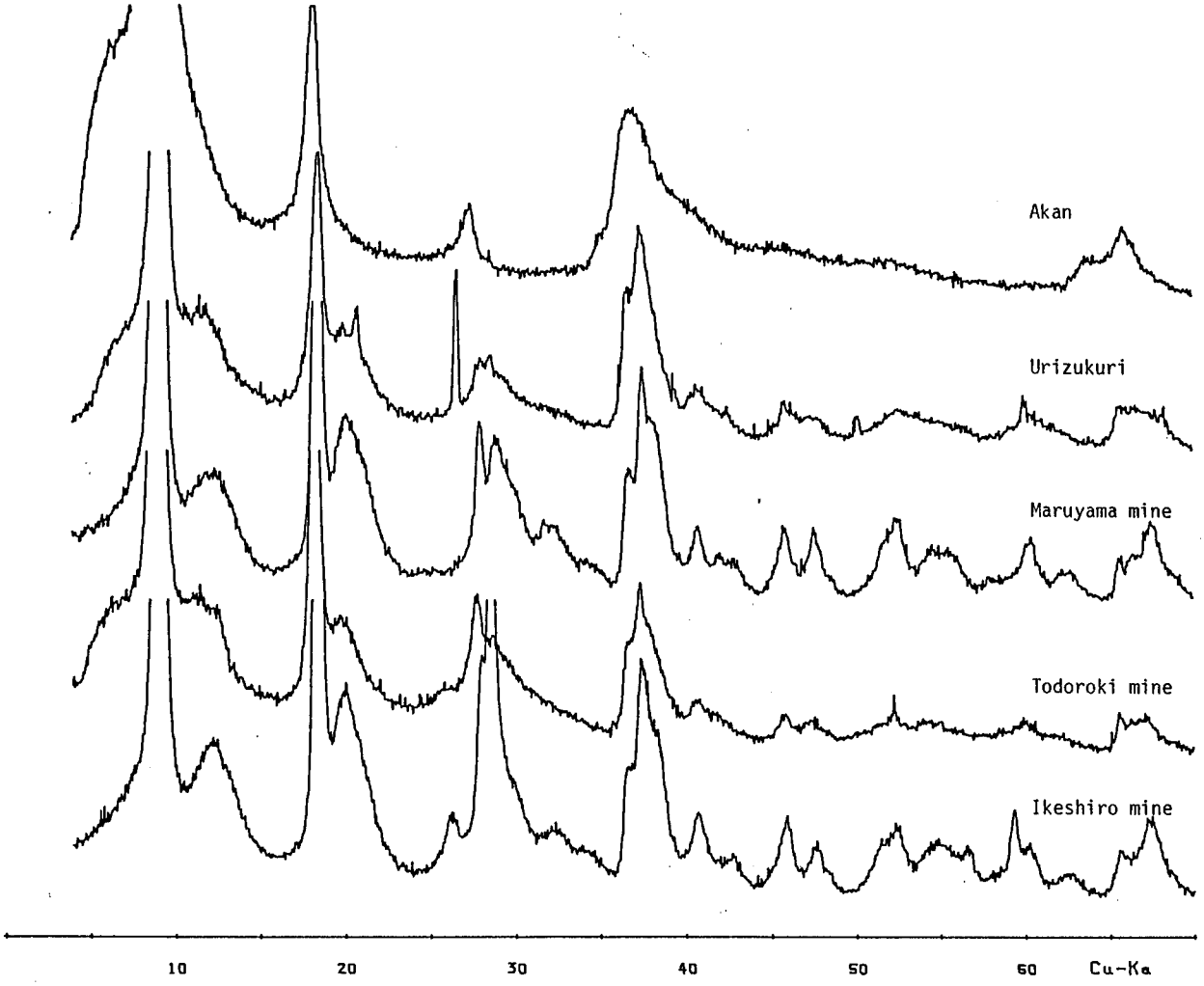

Fig.4 X-ray powder diffraction data of todorokite.
Full scale of vertical axis is 100 cps.
The diffraction peak of higher than 100 cps. are cut.
See Fig.3 for experimental conditions.

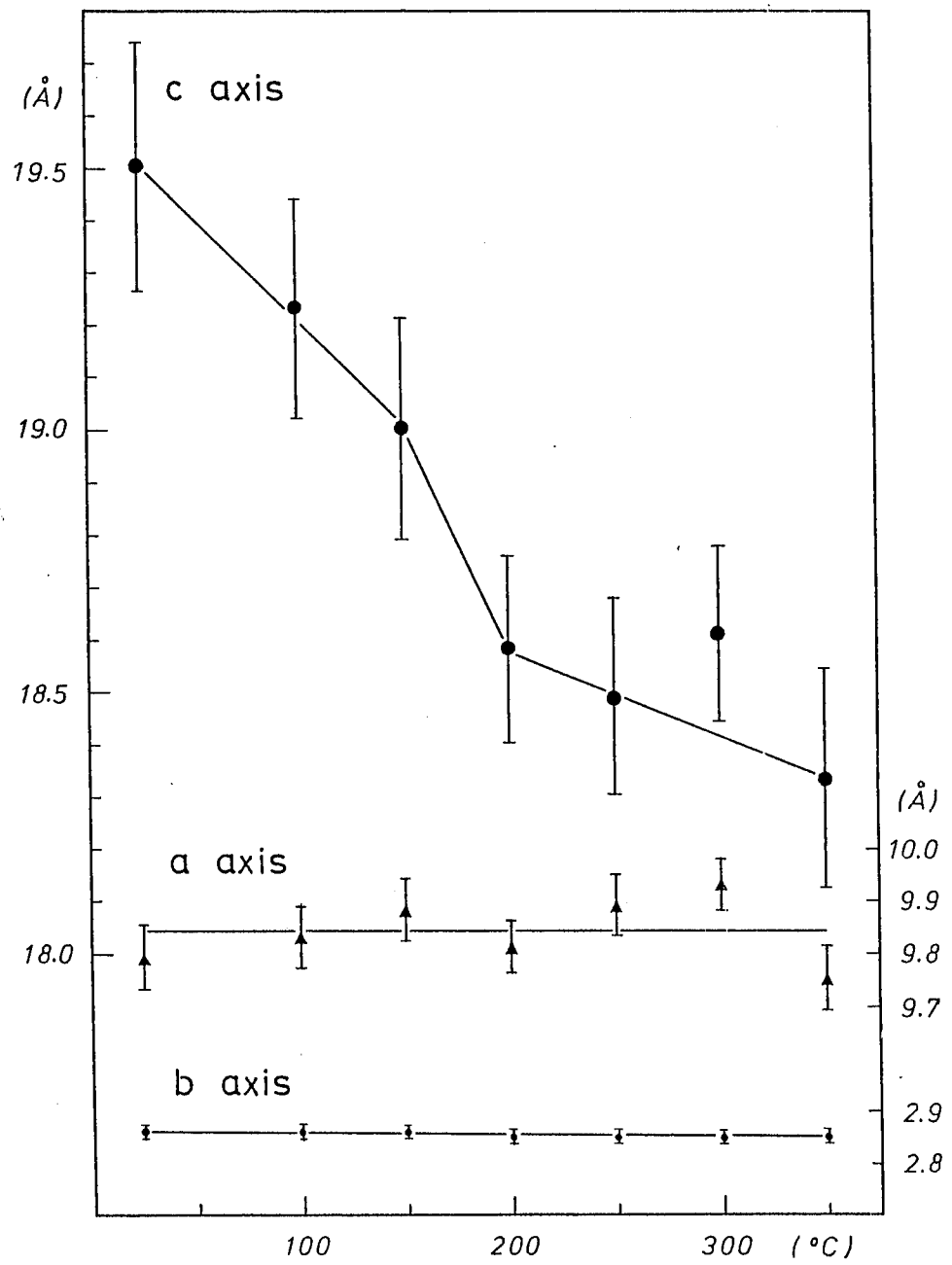

Fig.5 Temperature dependence of cell dimensions of todorokite which has superstructure.

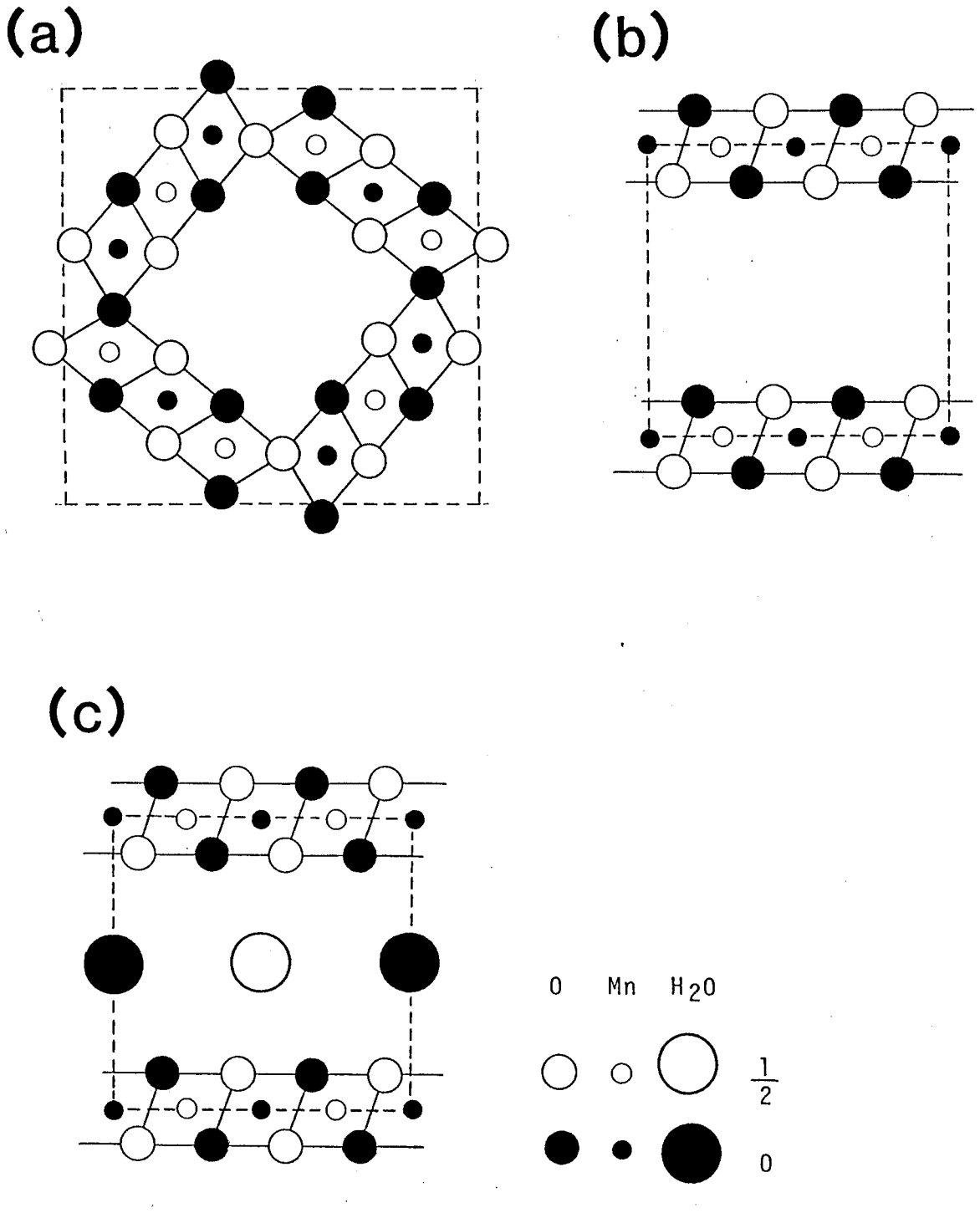

Fig.6 The crystal structure model used for calculation.
(a) 3x3 tunnel structure model.
(b) layer structure model.
(c) layer and bridge model.
layer model having H_2O between $[MnO_6]$ layer.

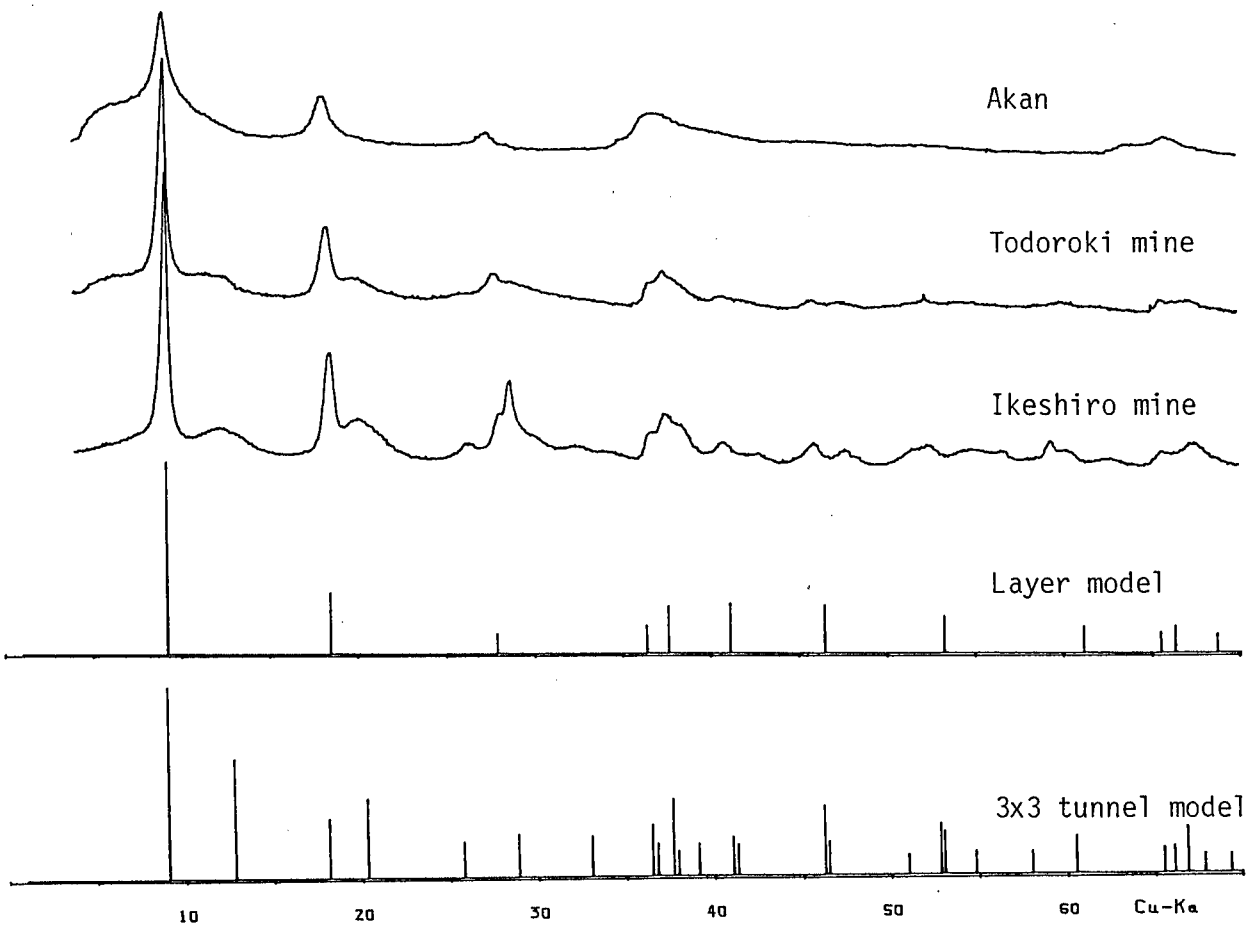

Fig.7 Comparison of x-ray diffraction data of natural todorokite and calculated results based on the 3x3 tunnel model and the layer model.
The intensity is expressed in terms of square root.

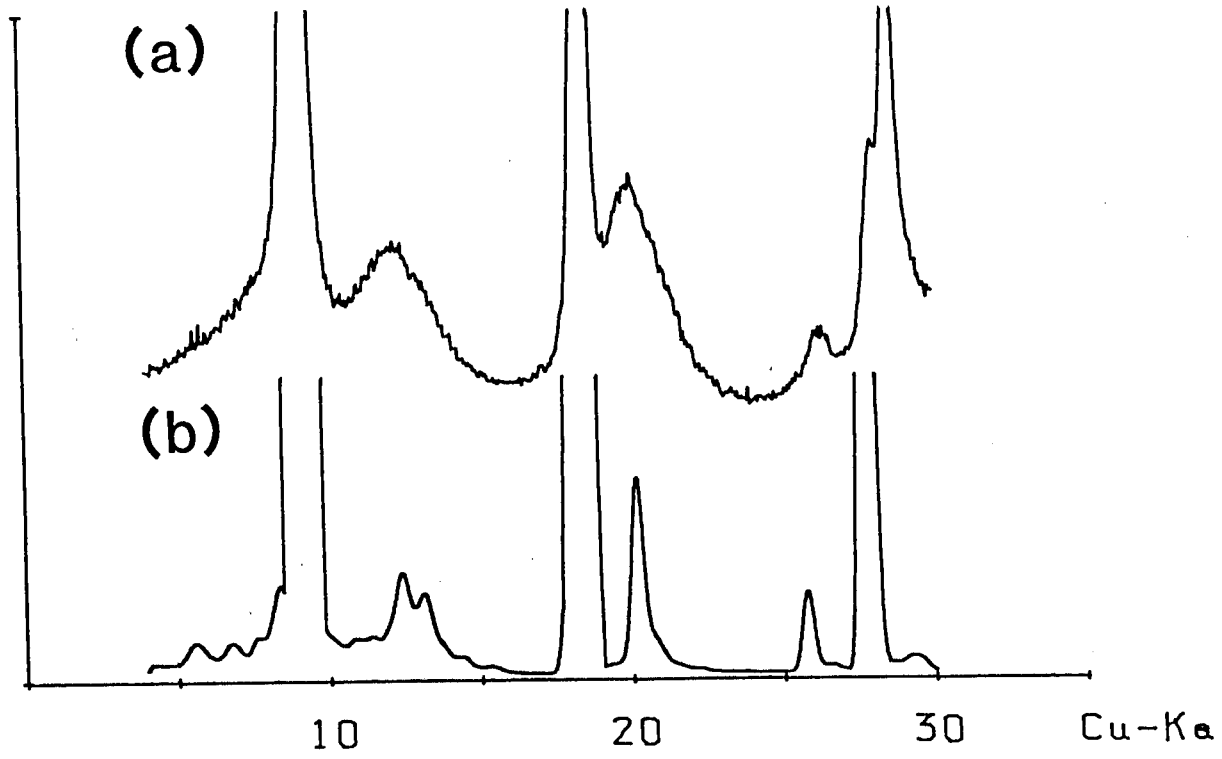

Fig.8 Comparison of x-ray diffraction profile.
(a) Todorokite from Ikeshiro mine.
(b) Calculated profile based on the layer and bridge model.

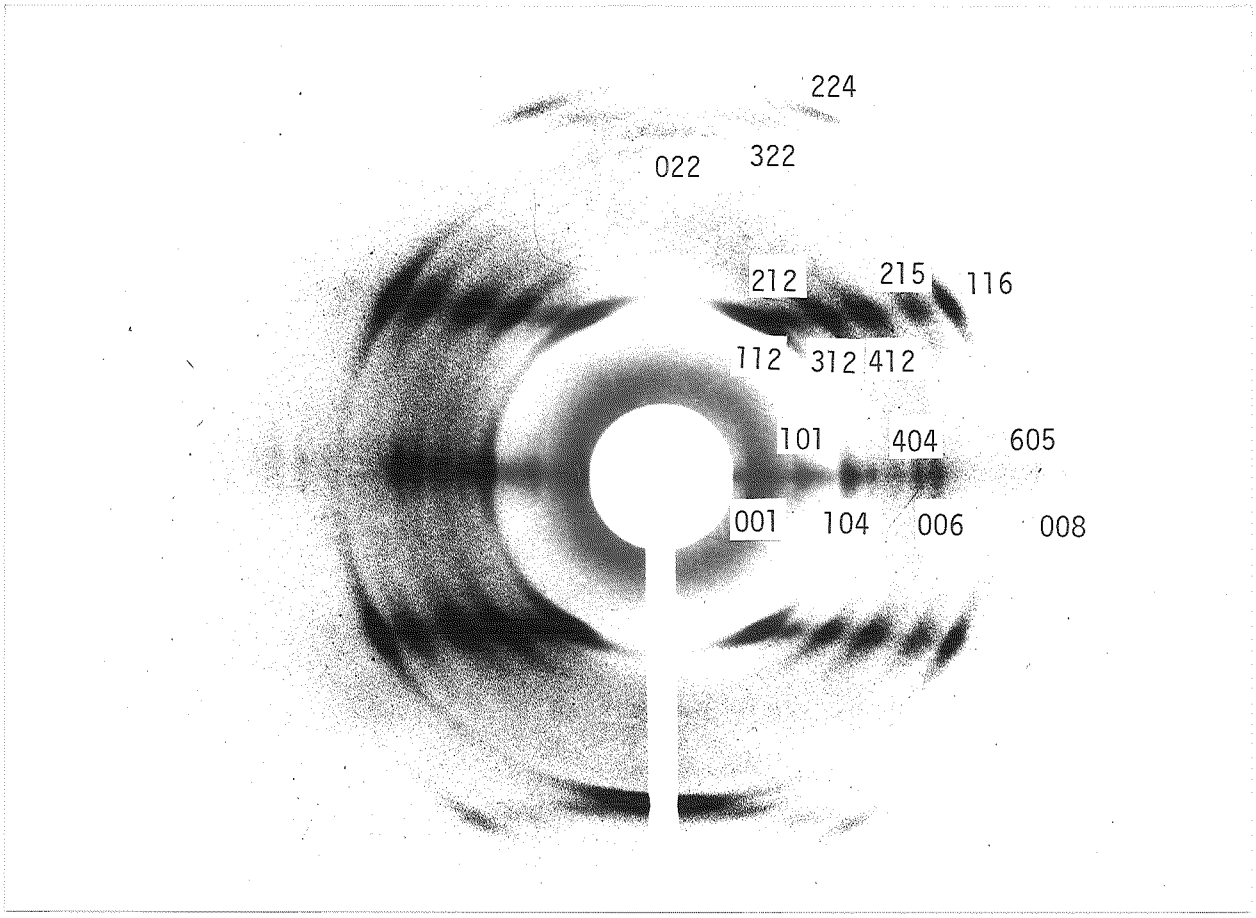

Fig.9-(a) X-ray diffraction photograph of acicular todorokite.
distance: 30 mm.

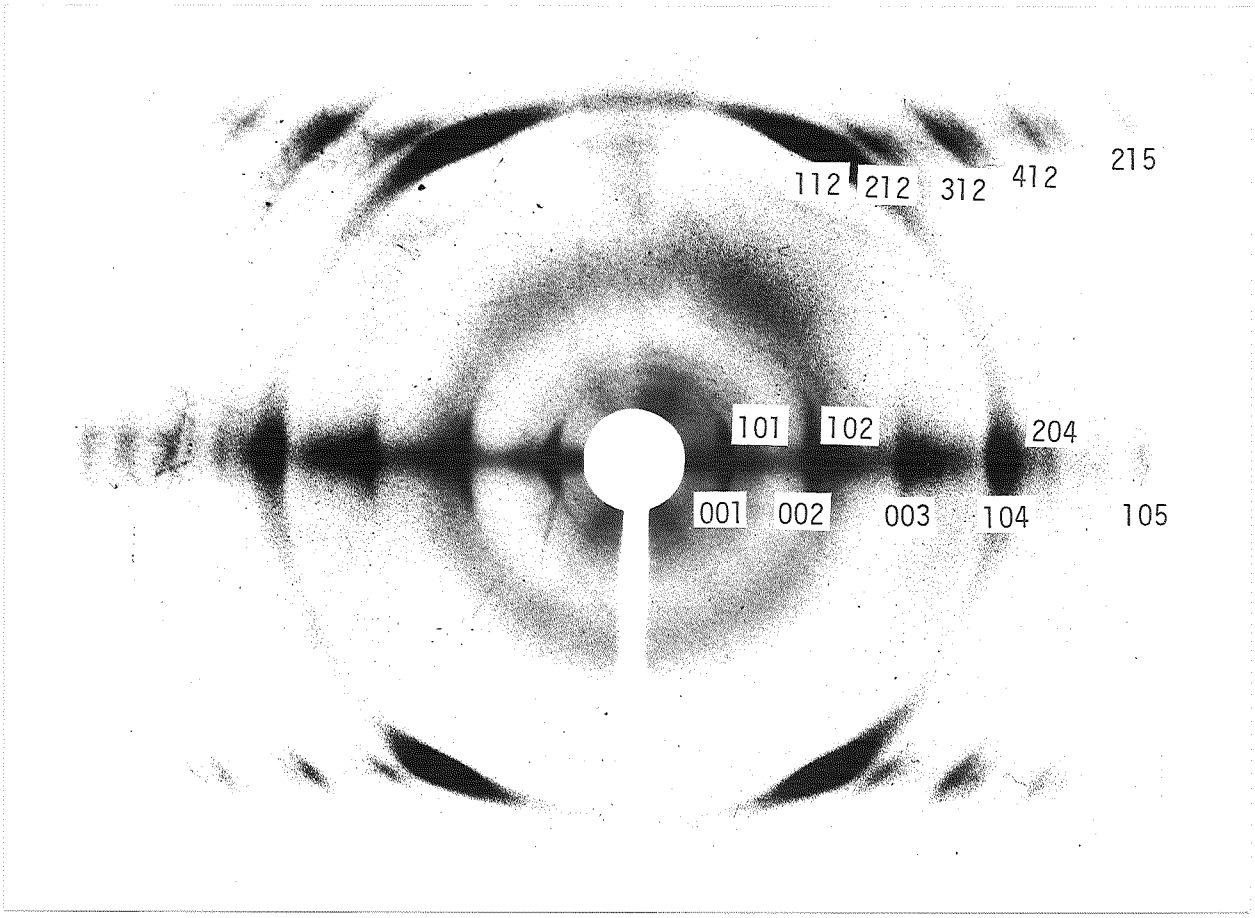

Fig.9-(b) X-ray diffraction photograph of acicular todorokite.
distance: 60 mm.

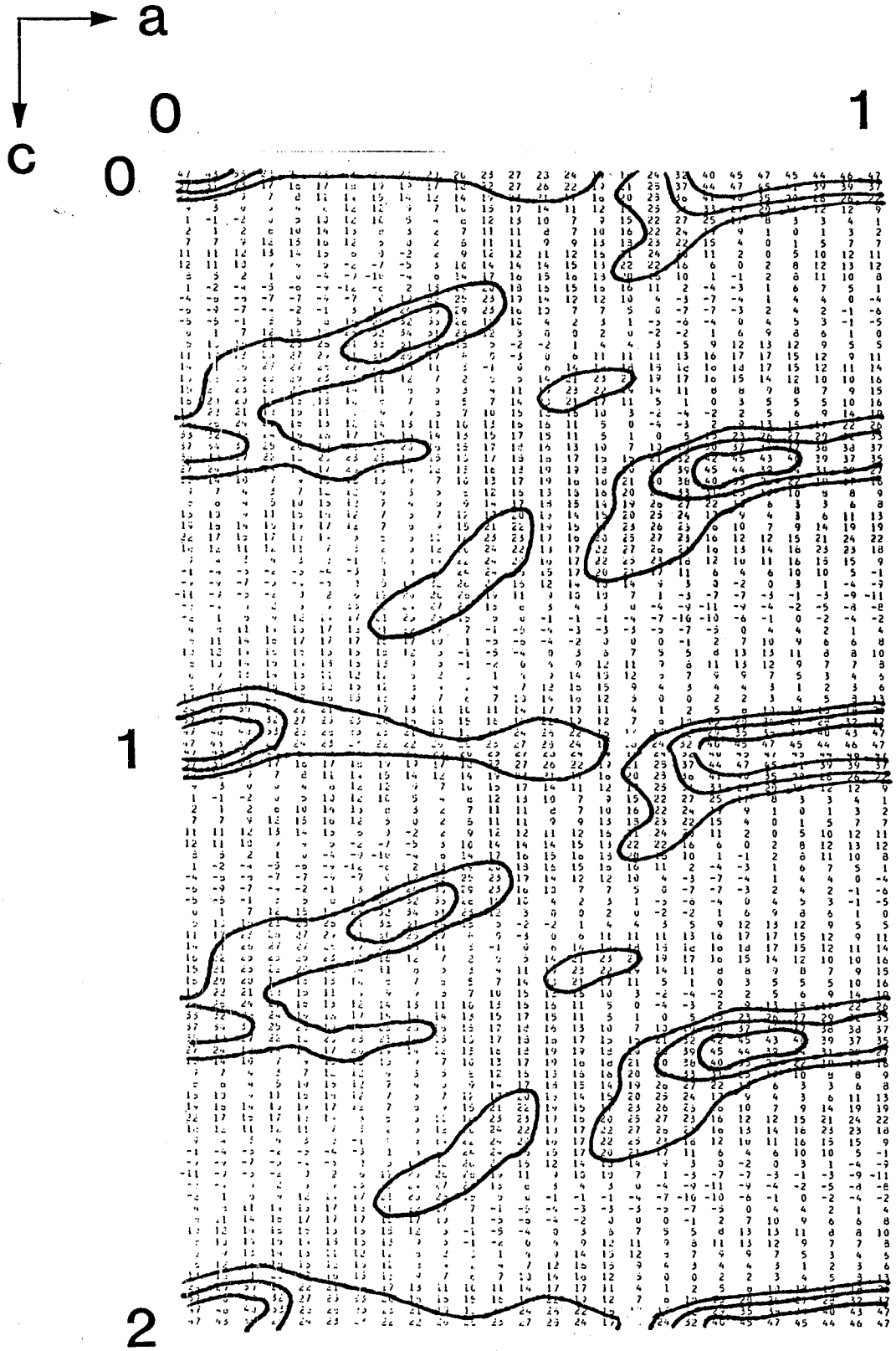

Fig.10-(a) Electron density section of acicular todorokite. parallel to (010), Y=0.

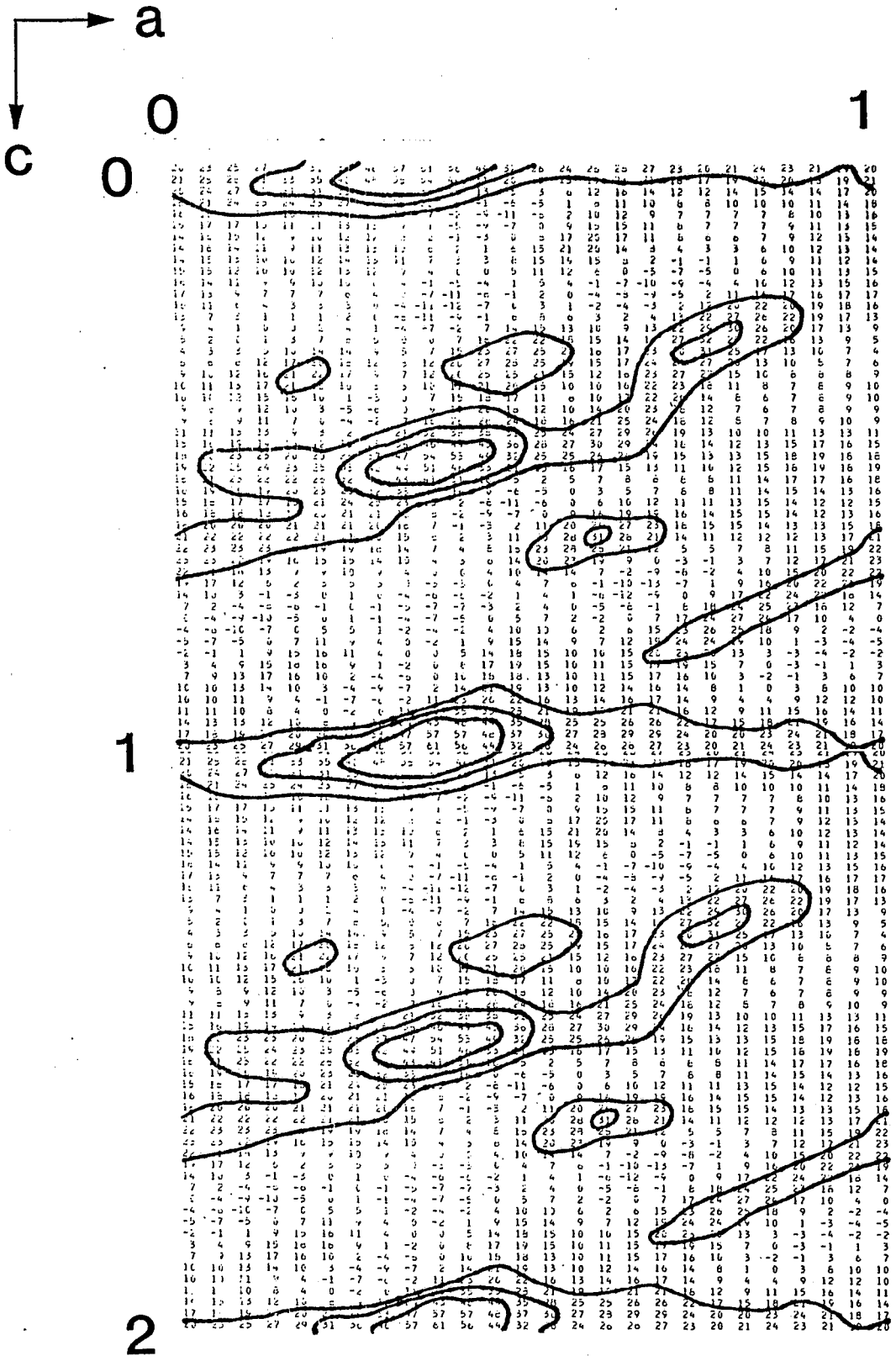

Fig.10-(b) Electron density section of acicular todorokite. parallel to (010), Y=1/2.

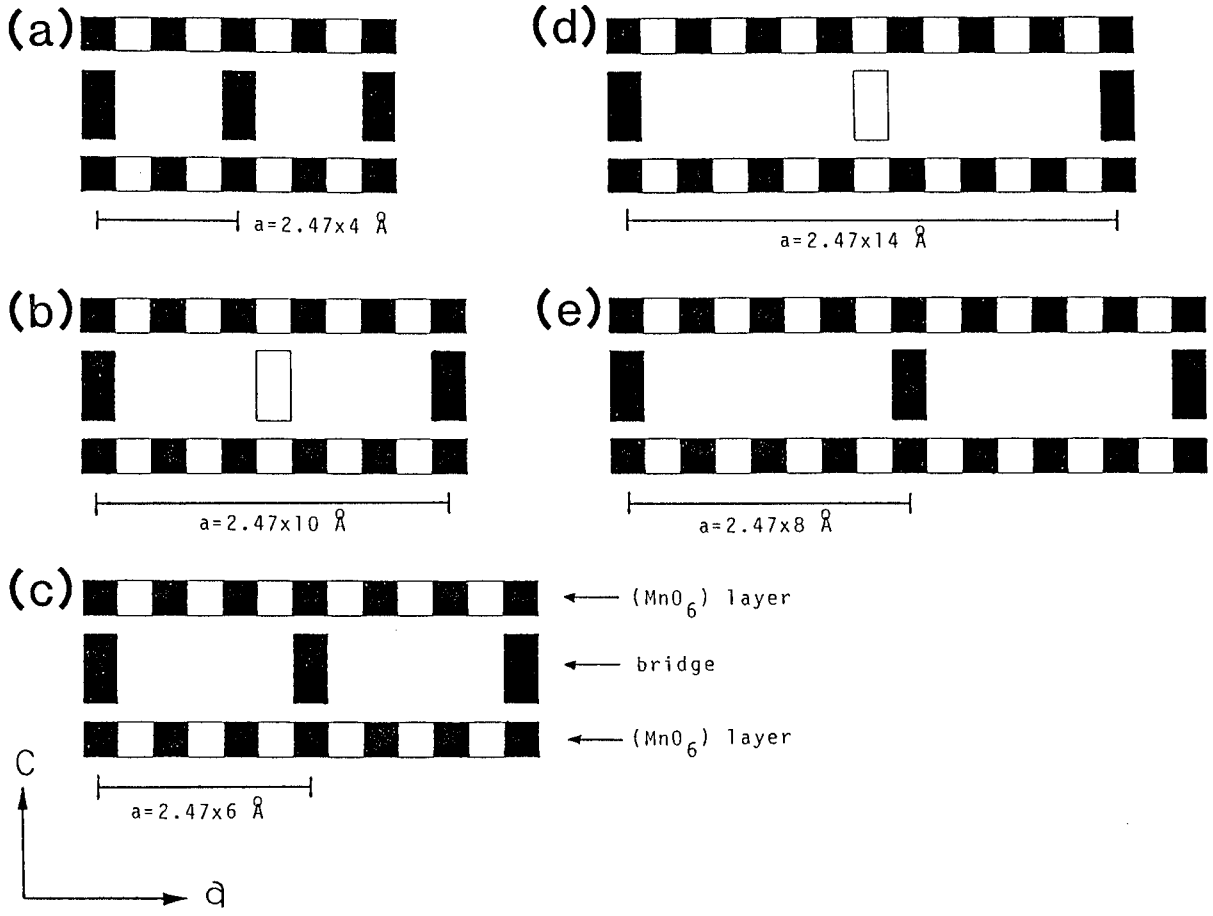

Fig.11 Schematic diagram of layer and bridge structure models.
The line below each model indicates the length of a-axis.
(a) a=9.87 Å (b) a=24.7 Å
(c) a=14.8 Å (d) a=34.5 Å
(e) a=19.7 Å
A small square represents [MnO_6] octahedron.
Rectangle represents bridge. Each octahedron shifts 1/2 b alternately as figured by white and black. A bridge can also shift 1/2 b depending on the position of [MnO_6].

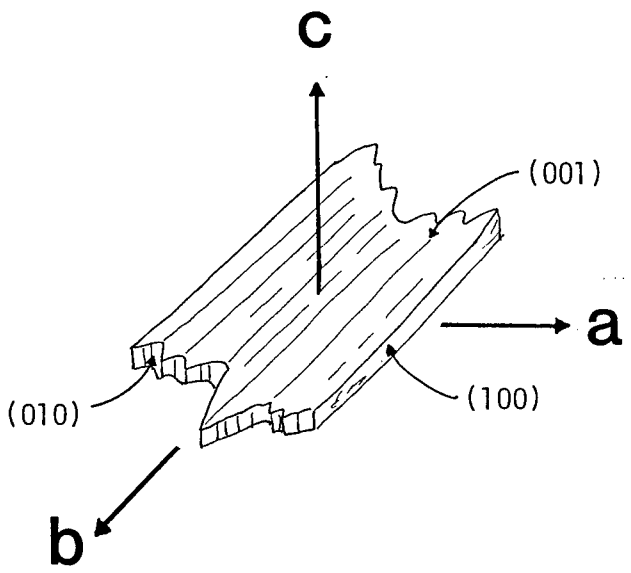

Fig.12 The relationship between crystal morphology and axial direction (after Straczek et al.,1960).
Todorokite specimens consist of narrow lathes or blades. The direction of b-axis is proved by the x-ray diffraction photograph of acicular specimen. The direction of c-axis is proved as the x-ray powder diffraction peaks of (001) become strong when samples are fixed to the holder with preferred orientation.
It has two cleavages parallel to (100) and (001). The nature of cleavages are different with direction. As todorokite is formed by the stacking of $[MnO_6]$ layer, it has a clear cleavage parallel to (001).